Solidification and Stabilization of Spent Pine-cone Biochar using Chemically Bonded Phosphate Cement

Shivani Tyagi[1] and *Ajit* Annachhatre[2*]
[1] Central University of Haryana, Mahendergarh, Haryana, 123029, India.
[2] Indian Institute of Technology, Mandi, Himachal Pradesh, 175005, India.
[*] Corresponding Author E-mail: ajit@iitmandi.ac.in

Abstract: Spent biochar is produced after adsorption of heavy metal which is hazardous by nature. A suitable disposal technique is required to prevent the leaching of heavy metals from spent biochar into the environment. This study highlights the solidification and stabilization (S/S) of copper loaded spent pine-cone biochar by chemically bonded phosphate cement (CBPC). The response surface methodology (RSM) was used to conduct S/S experiments in order to evaluate the compressive strength of CBPC products. The CBPC samples were prepared by varying biochar content (5-50 wt. %); W:S (0.15-0.3) and curing time(3-28d). Results illustrated that CBPC products containing biochar had higher compressive strength upto 12.8 MPa in comparison to CBPC without biochar i.e., upto 10.8 MPa. XRD and SEM analysis confirmed the presence of K-struvite ($MgKPO_4.6H_2O$), copper containing phases (Ca-Cu-Si), copper phosphate precipitates ($Cu_3(PO_4)_2$) and filling of pore spaces by spent biochar. Highest compressive strength of 12.8 MPa was obtained at an optimized biochar content of 25%, W:S of 0.18 and curing time of 28 d. The evaluation of leaching potential by TCLP illustrated that stabilization of Cu (II) upto 99.9% was achieved in CBPC product. The risk assessment study revealed that there is no significant danger due to leaching of heavy metals from final CBPC product indicating that it can be readily disposed in the hazardous landfill sites.

Keywords: *copper loaded biochar, hazardous waste management, phosphate binders, risk assessment studies, TCLP*

1. Introduction

The contamination of water bodies (surface water and groundwater) due to ingress of heavy metal is leading to environmental pollution worldwide because they are toxic, carcinogenic and bio-accumulative in nature [1]. Therefore, several techniques are used for the removal of from industrial effluents contaminated with heavy metals such as hydroxide and sulfide precipitation [2], ion exchange [3], adsorption [4] and photocatalytic processes [5]. Agricultural and forest residues which are considered as low cost and economical adsorbents can be used for heavy metal removal [6]. Agro-based adsorbents such as rice husk, corn-cob

and pine residues are reported to have good heavy metal adsorption capacities in the range of 6-12 mg/g [7]. Biochar is produced from pyrolysis of lignocellulosic biomass in an oxygen-limited environment is reported to have higher adsorption capacities in comparison to agricultural and forest residues [8, 9]. Recent studies have revealed that biochar produced from pine residues such as bark, needle and cone have superior copper adsorption capacities in the range 60 to 81 mg/g as compared to that of pine residues in the range of 9 to 11 mg/g. Higher adsorption capacity is attributed to the higher surface area upto 368 m^2 /g of biochar produced from pine residues [6,10].

Regeneration of spent biochar, incineration and hazardous landfills are possible options for disposal of spent adsorbent [11]. On the other hand, direct disposal of this spent adsorbent in landfills can lead to leaching which can be a potential cause of groundwater contamination [12].

S/S is one of the promising techniques for final disposal of spent biochar as it aims at stabilizing toxic and hazardous chemicals. S/S technique immobilizes heavy metal into the solid matrix thereby converting the waste into lesser toxic materials [13].

CBPCs are prepared by mixing acid phosphate and metal oxide e.g., MgO and $NH_4H_2PO_4$ along with heavy metal containing ground waste e.g., pollutant containing adsorbent, cement kiln dust, fly ash, slag etc., along with water [14, 15]. When water is added to CBPC, the phosphates and MgO dissociate to form struvite[16]. This struvite is considered as major building block for CBPC [17].

The final CBPC matrix contains heavy metal phosphates which are known to have lower solubility, resulting in the prevention of heavy metal leaching. CBPC binders exhibit lowest leaching of heavy metals in comparison to AAC and OPC [14]. It has been reported that use of phosphate as binder is very helpful in simultaneously stabilizing and solidifying the metal ions within the solid matrix as shown in the investigation carried out on the binding performance of phosphate and CaO binders [20]. MgO and KH_2PO_4 were used in the preparation of magnesium potassium phosphate (M-K-P) binders. Similarly, CaO and NaH_2PO_4 were used for preparation of calcium sodium phosphate (Ca-Na-P) binders [21]. These binders were then used for stabilizing waste ash containing mercury. It was observed that the use of M-K-P and Ca-Na-P binders resulted in effective immobilization of heavy metal [21,14].

The use of CBPC as binder for solidification and stabilization of spent biochar containing heavy metals was studied by various researchers. The leachability and analysis of risk assessment for the final S/S product was also carried out in few studies. The usage of biochar in cement composites is increasing lately, due to its ability in enhancing the physical properties of these composites. Previous studies have reported an improvement in the mechanical properties such as performance of cement composites incorporated with biochar as a result of extended hydration period of cement due to its improved water retaining ability [22]. The addition of biochar leads to an increase in compressive strength since these biochar particles are finer and act as filler material which increases the density and also blocks pores thus, assisting in S/S of heavy metals [23].

Accordingly, the objective of the present research is to develop an appropriate matrix for incorporation of heavy metal (Cu(II) ions) laden spent biochar. The effect of different factors such as time of curing, binder and biochar content on the strength of the spent biochar containing phosphate binder has been assessed. The leaching potential and the possible dangers arising due to leaching of Cu(II) has also been evaluated in the present study.

2. Methodology:

2.1 Chemicals for S/S experiments

Analytical grade chemicals with purity greater than 90% were used in preparation of CBPC included calcium oxide (95%), magnesium oxide (95%), potassium dihydrogen phosphate (99%), sodium dihydrogen phosphate (99%) and ammonium dihydrogen phosphate (98%) obtained from Sigma Aldrich. DI water was used for preparation of samples in S/S experiments.

2.2 Design of experiments of S/S

Using the central composite design (CCD) method, experiments were designed to solidify and stabilize pine cone spent biochar. The CCD included 2^k factorial runs and 2k axial runs, where k represents the number of parameters, and also included n0 center points. The low levels of independent variables were coded as -1, while high levels were coded as +1. The study focused on three independent parameters: biochar content (5-50 wt.%), water to solid ratio (0.15-0.3), and curing time (3-28 d). The study had 8 factorial points, 6 replicates of the central point, and 6 axial points. A total of 20 experimental runs were conducted, determined by the following equation.

$$N = 2^k + 2(k) + n_0 = 2^3 + 2(3) + 6 = 20 \quad (1)$$

Here,

N: number of required experiments
k: factors/parameters
n_0: replicate of central points

Table 1. Process parameters of solidification and stabilization experiments

Parameter	**Factor**	**Uncoded values**		
		-1	0	+1
Curing time (d)	A	3	15.5	28
Biochar content (%)	B	5	27.5	50
W:S	C	0.15	0.325	0.5

The process parameters of solidification and stabilization experiments are shown in Table 1. The obtained experimental data was fitted using a quadratic model. The interaction effect of different factors on the important property of Compressive strength was studied using response surface methodology (RSM). Design Expert 13 was used to analyze the data and find a relation between the process parameters and compressive strength. Analysis of variance (ANOVA) was also used for analysis of process parameters.

2.3 Stabilization procedure

The S/S of pine cone spent biochar was carried out by using CaO, MgO and dihydric phosphates (KH_2PO_4, NaH_2PO_4 and $(NH_4)H_2PO_4$) as binders. Initially, these binders were homogeneously mixed in different ratios ratio in a borosilicate glass vessel. After mixing, the biochar was added to the mixture and water was then added in water: solid ratio of 0.15-0.3. A homogenous mixture was obtained by mixing all the components properly on a flat and dry surface. This mixture was transferred carefully into cast iron square molds of size

50mm×50mm×50mm. The samples were cured for durations of 3 days, 7 days, and 28 days. The CBPC samples were carefully demolded after leaving them untouched for a period of 24 hours. The characterization of final CBPC products was done by using SEM and XRD. CBPC products were also tested for analyzed for UCS, water absorption, leaching and stabilization of Cu (II). Several factors such as properties of the raw materials used, binder content, biochar content, liquid-to-solid ratios and curing time of samples was found to have influence on the strength of CBPC. Therefore, the effect of different factors on Compressive strength was studied by varying all these factors. The biochar content was varied from 5-50 wt % of binder content wt., curing time was kept at 3d, 7d and 28 d, 4 different binder compositions i.e 1:1:1, 0.5:1:1, 1:0.5:1, 1:1:0.5) for CaO: MgO: K_2HPO_4; were used, three different type of phosphate salt (K_2HPO_4, NaH_2PO_4 or $(NH_4)H_2PO_4$). W:S was varied from 0.15-0.3 and the effect on UCS was evaluated. Boric acid (0.3% by wt of solids) was added as a retarder. CBPC samples were prepared by varying the biochar content from 5-50% by wt. The S/S samples were prepared and tested in triplicates. The average compressive strength of the triplicates was considered for further calculation.

2.4 Characterization of CBPC product

CONTROLS Compressive strength testing machine having a maximum load capacity of 1,000 N. was used for carrying out UCS tests on all the CBPC products. The maximum compressive strength of each sample was calculated individually dividing the maximum load just before cracking with the cross-sectional area. The final CBPC products were also tested for water absorption [24]. Surface characterization of CBPC samples was carried out using EDX-SEM. Surface morphology of the CBPC final products was studied using SEM images. The composition of CBPC samples was determined by using EDX.

2.5 Leaching Study

Toxicity characteristic leaching procedure (TCLP) was used for determining the heavy metal leachability from CBPC products. For this purpose,10 mL of 0.1 M acetic acid was added to 1 g of CBPC product in a 50 mL laboratory flask. A rotary incubator shaker was used to agitate this mixture for a period of 18 h and the rotations of the shaker were fixed as 32 rpm. A nylon filter of 0.25 microns was used to then filter this mixture. The analysis for heavy metal content of the filterate thus obtained was done by using AAS. The formulae used for calculating the value of maximum leaching and stabilization were as follows [25]:

$$\text{Maximum Leaching value} = \frac{(\text{Heavy metal content} \times 0.1)}{\text{TCLP extraction Fluid Volume}} \quad (2)$$

$$\text{Stabilization (\%)} = \frac{(Maximum\ leaching\ Value - TCLP\ value)}{Maximum\ leaching\ Value} \times 100 \quad (3)$$

2.6 Risk Assessment Study

The assessment of the risk to the ecology and humans are the major parameters to determine the potential hazards of heavy metals [24]. The risk assessment of the ecological factors is evaluated by using a Contamination factor (C_f). Contamination factor (C_f) is used to determine the amount of heavy metal contamination in a leachate (Eq. 4) [26]:

$$C_f = \frac{C_{Leachate}}{C_{Total}} \quad (4)$$

The assessment of risk to humans is evaluated by determining the possible carcinogenic and non-carcinogenic effects of heavy metal exposure on the health of humans. The major elements for assessment of risks to human health include hazard quotient, Assessment of exposure to heavy metals and hazard index and. The assessment of exposure to heavy metals by direct contact with leachate through touch or skin or due to ingestion was determined as follows [27]:

$$E_{ingestion} = \frac{C_{Leachate} \times I_R \times E_F \times E_D \times 10^{-6}}{B_W \times A_T} \quad (5)$$

$$E_{dermal} = \frac{C_{Leachate} \times S_A \times A_F \times A_B \times E_D \times E_F \times 10^{-6}}{B_W \times A_T} \quad (6)$$

For the various factors such as A_B, SA, E_D and A_F in equations (5) and (6) the values were obtained from the previously reported literature [28, 29]. The data on exposure to heavy metals was used for calculation of the hazard index as [24]:

$$HQ_{ingestion/dermal} = \frac{E_{ingestion/dermal}}{R_D} \quad (7)$$

$$HI = \frac{\sum_{i=1}^{n} HQ}{n} \quad (8)$$

The values of R_D for Cu (II) were obtained from the previously reported literature [28, 29].

3. Results and discussion

3.1 Selection of binder:

Three different binders were synthesized by using different types of phosphate salts: (i) KH_2PO_4 binder, (ii) NaH_2PO_4 binder, and (iii) $(NH_4)H_2PO_4$ binders. The analysis of UCS and water absorption (%) was carried out to determine the binding capacity of these phosphate salts. The two most important parameters for determination of the products quality include UCS and water absorption (%). UCS measures the strength of the final products depends on the binding capacity of these phosphate binders and the spent adsorbents. Water absorption (%) is used to evaluate the performance and quality of the final product in moist areas and environments with high humidity. Fig. I brings out that K_2HPO_4 provided maximum strength to the matrix at all the three binder ratios followed by NaH_2PO_4 and $(NH_4)H_2PO_4$. Moreover, the water absorption (%) obtained for KH_2PO_4, $Na_2H_2PO_4$ and $(NH_4)H_2PO_4$ was 21.6%, 52.4% and 36.5% respectively. As seen in Fig. 1, NaH_2PO_4 and $(NH_4)H_2PO_4$ showed high water adsorption capacity (52.4%) and 36.5% respectively as compared to KH_2PO_4 based binders (21.6 %).Thus, NaH_2PO_4 and $(NH_4)H_2PO_4$ was not suitable in comparison to KH_2PO_4 based binders. Similar results were reported by previous researchers [29, 30]. Therefore, KH_2PO_4 was used for further experiments.

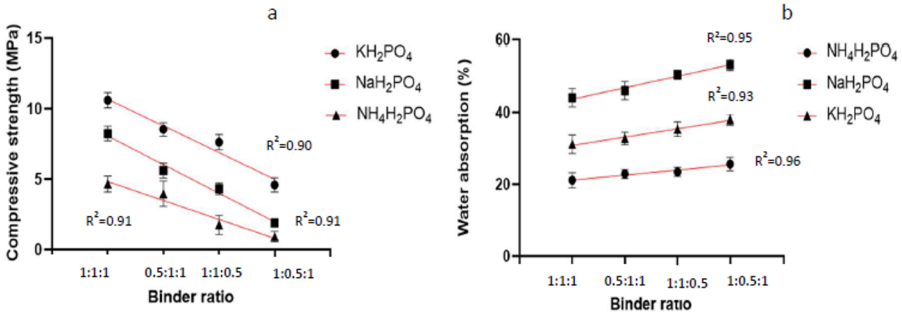

Fig. 1. Effect on binder ratio (wt. %) on (a) compressive strength and (b) water absorption

3.2 Effects of compositions of binders

There are three main constituents in CBPC binders viz. CaO, MgO, K_2HPO_4. Four different ratios, (A) 0.5:1:1; (B) 1:0.5:1; (C) 1:1:0.5 and (D) 1:1:1; and were used by varying one constituent and keeping the others same. As Fig. 2 reveals, the compressive strength for ratio A (1:1:1), was found to be maximum and for ratio D, it was found to be minimum. The order of the compressive strength for different ratios was: D > C > A > B. As can be seen in the (Fig. 2), the effect of CaO and KH_2PO_4 on the compressive strength (α) was not significant. The α reduced due to reduction in MgO content. This clearly shows the importance of MgO in the S/S of CBPC products. The same was reported in previously documented research observations [31]. The minimum value for the UCS tests as per AS4455 (for solid or cored masonry units), is 3.5 MPa. The results in the present study were found to meet the prescribed value for UCS tests. The ratio A (1:1:1) depicted maximum value of UCS and was hence used for conducting the experiments in present study.

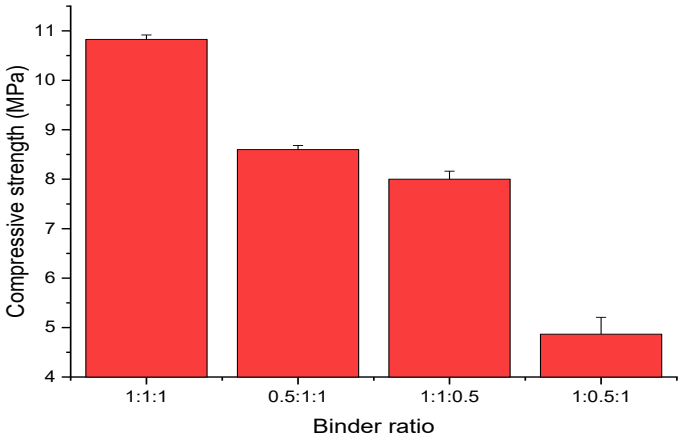

Fig. 2. Effect on compressive strength due to binder ratio (%)

3.3 Interaction of operational parameters on compressive strength of CBPC product:

The CBPC's compressive strength (measured in MPa) was assessed through S/S experiments employing the CCD technique. The curing time (ranging from 3-28 days), W:S ratio (between 0.15-0.3), and biochar content (ranging from 5-50 wt. %) were varied to analyze the independent impact of each factor on compressive strength, as demonstrated in the all-factor interaction plots (Fig. 3). To examine the effect of all factors on compressive strength, response surface methodology was employed (Fig. 3).

3.3.1 Impact of operational parameters on compressive strength:

Fig 3(a) shows that with increase in curing time from 3 to 28 d, the value of compressive strength increased from 4 to 12.8 MPa. For biochar dosage up to 25 % compressive strength increased but with further increase in biochar content (i.e. more than 25%) the compressive strength reduced to 6.9 MPa. The maximum compressive strength of 12.8 MPa was obtained at biochar content of 25% (Fig. 3 b). With increase in W:S, a decrease in compressive strength was observed (Fig. 3 c).

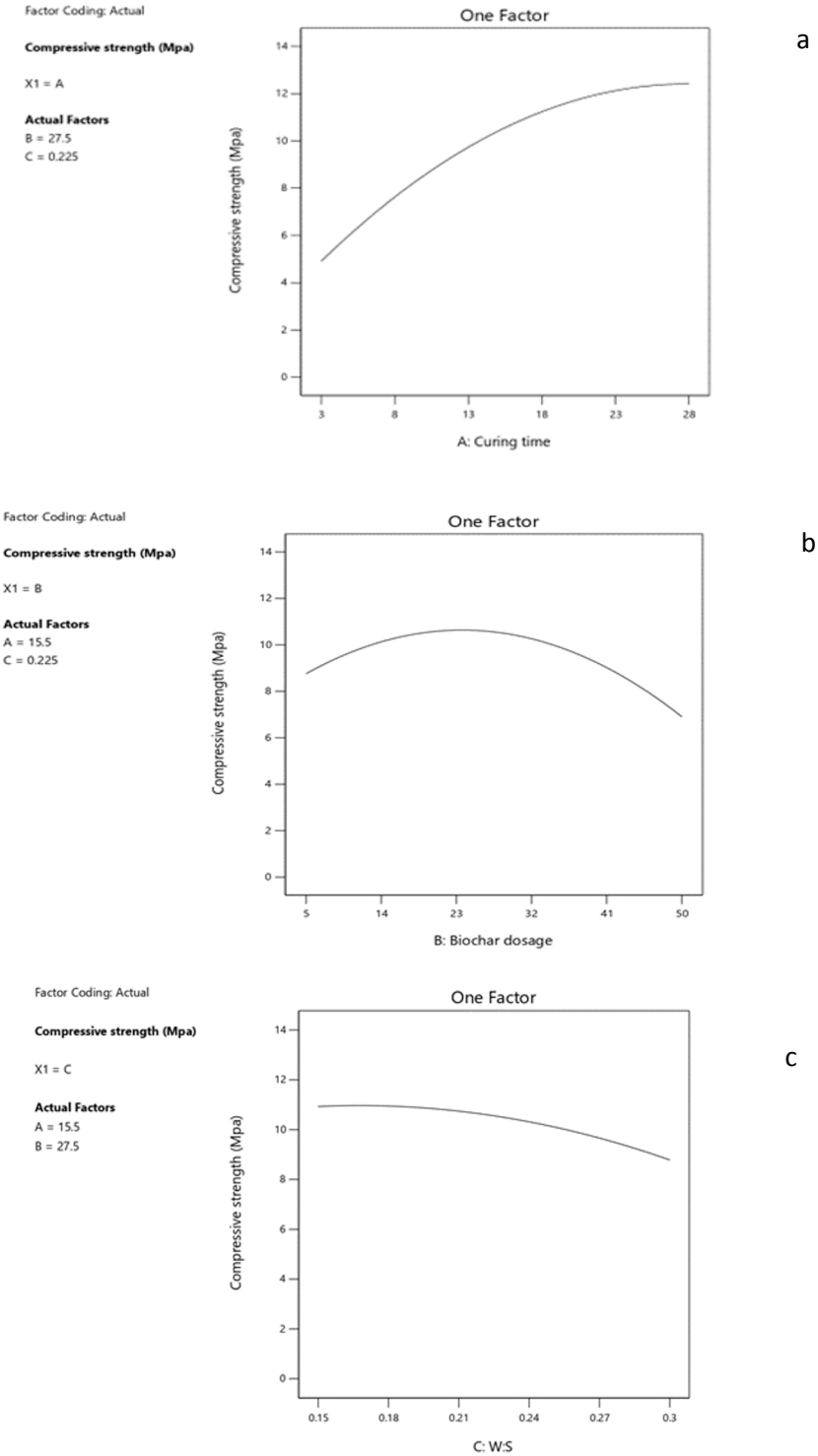

Fig. 3. All effect interaction plots of operational parameters (a) curing time, (b) biochar content and (c) W:S

3.3.2 Surface and contour plots

The Figure 4(a) demonstrate the combined influence of W:S ratio, curing time, and biochar content on compressive strength through surface plots in a three-dimensional view. The maximum compressive strength of 12.8 MPa was achieved when the W:S ratio was 0.2 and the biochar content was 25%. The compressive strength increased as the biochar content increased up to 25%, but it decreased with further increases in biochar content. Previous studies have reported similar findings where the addition of fly ash led to increased compressive strength due to the filling of pore spaces and the emergence of new binder phases [32, 20]. In Figure 4(b), it can be observed that the compressive strength increased as the curing time increased from 3 to 28 days. A maximum compressive strength of 12.8 MPa was observed after 28 d of curing. This compressive strength is higher than then the minimum recommended value of 3.5 MPa as per various regulatory organizations such as US Nuclear Regulatory Commission Standard and ASTM (C62) standard [33]. The accuracy of the obtained model was verified by comparing the calculated value and predicted value (Table 2).

Table 2. Calculation through model equations

Uncoded			**Coded**					
A:Curing time	**B:Biochar dosage**	**C:W:S**	**A:Curing time**	**B:Biochar dosage**	**C:W:S**	**Calculated value**	**Actual Value**	**Predicted Value**
15.5	27.5	0.225	0	0	0	10.56	11.1	10.56
28	27.5	0.225	1	0	0	12.41	10.6	10.56
3	5	0.3	-1	-1	1	0.708	12.4	12.41
28	50	0.15	1	1	-1	8.498	10.32	10.56
28	5	0.3	1	-1	1	9.483	0.62	0.6987
3	27.5	0.225	-1	0	0	4.91	4.8	4.91
15.5	27.5	0.225	0	0	0	10.56	10.55	10.56
15.5	5	0.225	0	-1	0	8.765	8.8	8.76
3	50	0.15	-1	1	-1	2.273	0.5	0.3287
15.5	27.5	0.225	0	0	0	10.56	11.68	11.82
15.5	27.5	0.3	0	0	1	8.7905	8.65	8.79
15.5	27.5	0.225	0	0	0	10.56	2.72	2.64
15.5	27.5	0.225	0	0	0	10.56	6.75	6.91
3	5	0.15	-1	-1	-1	2.643	10.95	10.93
15.5	50	0.225	0	1	0	6.915	2.2	2.27
15.5	27.5	0.225	0	0	0	10.56	10.8	10.56
28	5	0.15	1	-1	-1	6.828	6.09	6.14
10	33	0.18	-0.44	0.24	-0.6	8.6		

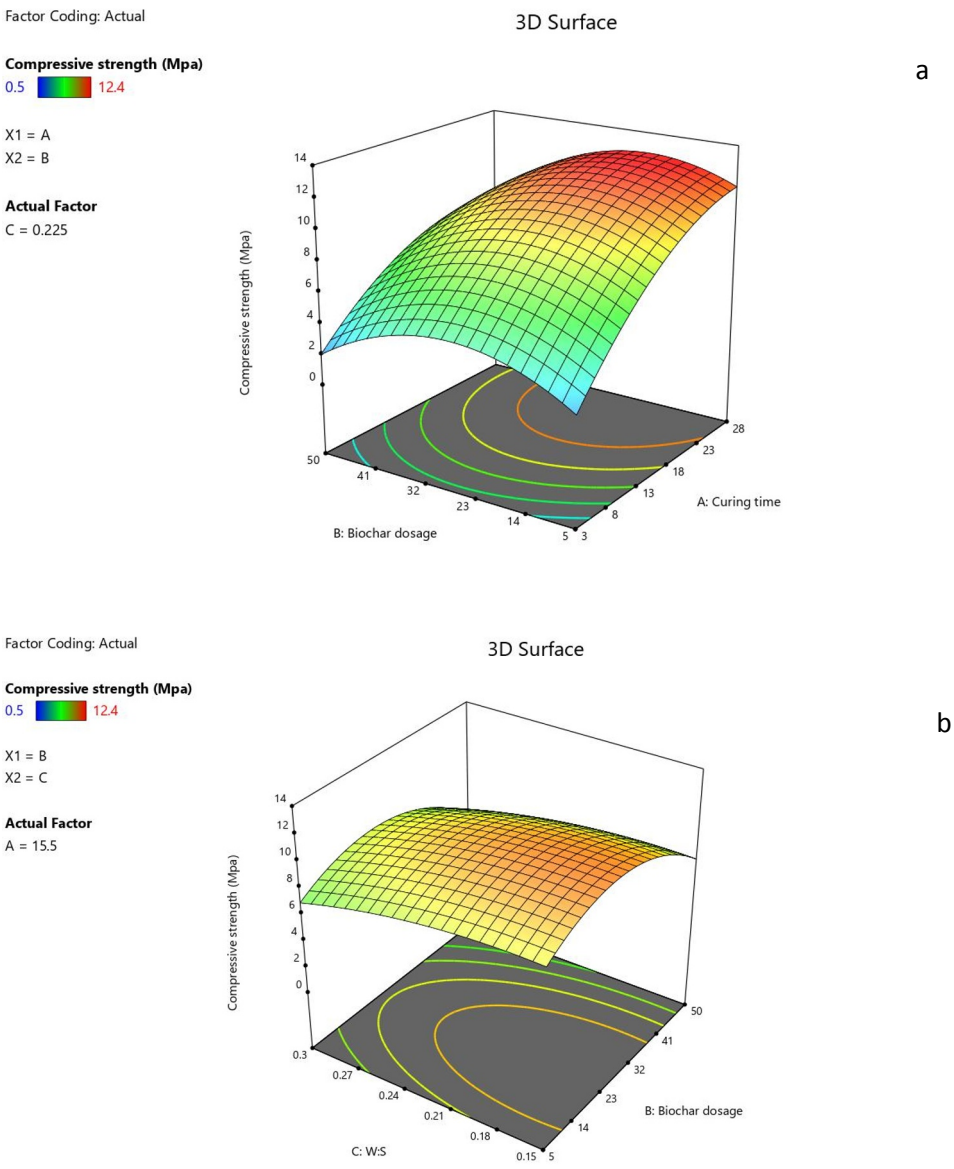

Fig. 4. 3-D surface and contour plots showing effect on compressive strength due to (a) biochar dosage (%) and (b) W:S and Curing time

3.9 Model equations and analysis of variance of compressive strength:

Table 3. Analysis of variance of compressive strength of CBPC sample

	Sum of Squares	df	Mean Square	F-value	p-value	
Model	273.20	9	30.36	441.68	< 0.0001	significant
A-Curing time	140.63	1	140.63	2046.11	< 0.0001	
B-Biochar content	8.56	1	8.56	124.49	< 0.0001	
C-W:S	11.49	1	11.49	167.21	< 0.0001	
AB	4.38	1	4.38	63.74	< 0.0001	
AC	0.0841	1	0.0841	1.22	0.2947	
BC	0.0000	1	0.0000	0.0000	1.0000	
A^2	9.92	1	9.92	144.38	< 0.0001	
B^2	20.41	1	20.41	297.02	< 0.0001	
C^2	1.35	1	1.35	19.58	0.0013	
Residual	0.6873	10	0.0687			
Lack of Fit	0.1565	5	0.0313	0.2949	0.8968	not significant
Pure Error	0.5308	5	0.1062			
Cor Total	273.89	19				
Adjusted R^2	0.99					
Predicted R^2	0.98					

The compressive strength of spent pine cone biochar was examined using the CCD under RSM technique to identify the optimal conditions. Table 3 presents the compressive strength analysis of the S/S experimental data. From Table 3, it can be observed that the P-value for curing time, W:S, and biochar content is less than 0.0001, indicating their significance. The R^2 for the S/S experiments was 0.99, which suggests that the model can be employed to investigate the interaction of various factors, such as curing time, spent biochar content, and W:S, on compressive strength.

Design Expert 13 software was employed to analyze the results. The quadratic model was used to determine the impact of curing time (A), biochar content (B), and W:S (D) on compressive strength. Thus, the following equation were obtained:

$$\text{Compressive strength (MPa)} = 10.56 + 3.75A - 0.9250B - 1.07C - 0.7400AB - 0.1025AC - 1.90A^2 - 2.72B^2 - 0.6995C^2 \quad (9)$$

The significance of the terms in equation (9) was determined using the factor coefficients. The constant values in equation (9) represent the compressive strength when the impact of other parameters is ignored. For example, in equation (16), a constant value of 10.56 indicates the compressive strength when the influence of other operating parameters is not considered. Using the value of operating parameters, such as curing time, W:S, and biochar content, equation (9) can be used to predict compressive strength (C). For instance, as demonstrated in Table 4, for the operating uncoded values shown in Col. 2, the values can be transformed into coded values through interpolation. Further, by utilizing the values in equation (9), compressive strength can be calculated, resulting in 8.6 MPa.

Table 4. Uncoded and coded values

Parameters	Uncoded	Coded
A (Curing time)	10 d	-0.44
B (biochar content)	33	0.24
C(W:S)	0.18	-0.6

Equation (9) breaks down compressive strength into three linear terms (A, B, and C), three two-effect terms (AB, AC, and BC), and three quadratic terms (A^2, B^2, and C^2). According to Table III, the significant terms for obtaining maximum compressive strength are A, B, C, AB, A^2, and B^2. In the present investigation, A^2 and B^2 were deemed significant (P-value <0.001), indicating their considerable effect on compressive strength.

3.5 Phases present in CBPC product:

The mineralogy for the bulk phase of CBPC product was done by using X-ray diffraction (XRD) analysis. The diffraction angles (2θ) of the samples was observed and various phases were identified using X'pert Highscore software by diffraction cards of Joint Committee on Powder Diffraction Standards (JCPDS). Fig. V shows the XRD spectra of CBPC product with varying biochar contents (5%, 25% and 50%). The formation of $MgKPO_4{\cdot}6H_2O$ was confirmed by diffraction peaks at 2θ = 19°, 38° and 61° [34]. The formation of $MgKPO_4{\cdot}6H_2O$ due to participation of PO_4^{3-}, Mg^{+}, Ca^{2+} and K^{+} ions released by the dissolution of KH_2PO_4, CaO and MgO through the following reaction [21]:

$$Mg^{2+} + PO_4^{3-} + K^{+} + 6H_2O \rightarrow MgKPO_4.6H_2O \qquad (10)$$

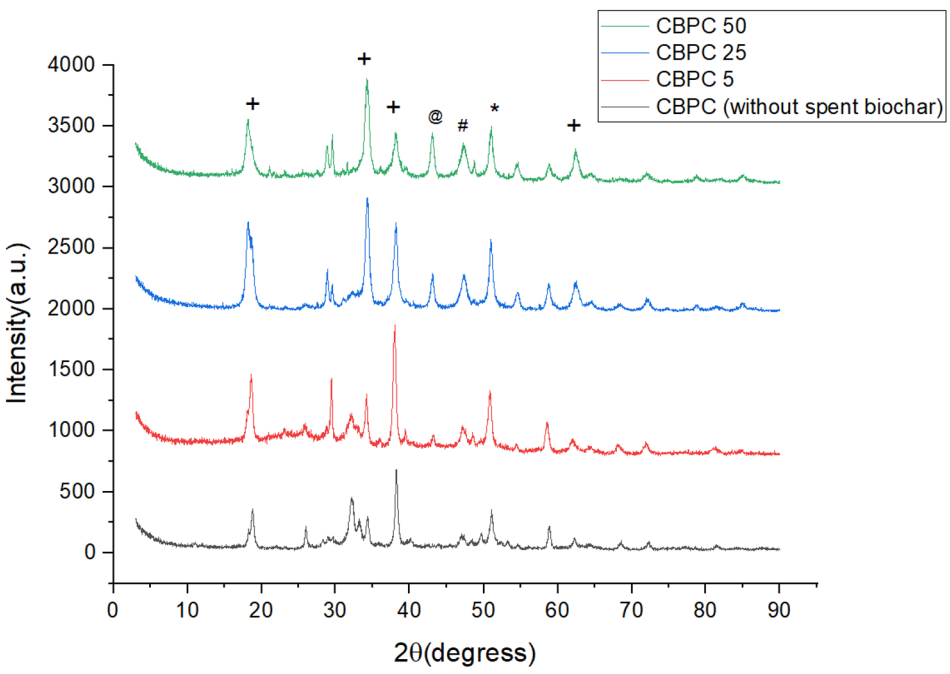

Fig. 5. XRD spectra of the CBPC product

Fig. 5 reveals that there was a gradual increase in the diffraction peaks intensity of $MgKPO_4 \cdot 6H_2O$ due to increase in the biochar content, but the same for MgO were almost similar, this pattern is also confirmed by other researchers [35]. The mineralogical (XRD) analyses revealed that CBPC product comprise of phosphate-based precipitates such as $MgKPO_4$, $Cu_3(PO_4)_2$ at $2\theta=38^o$ and 48^o, respectively [36]. Similar results have been reported by previous research [37]. Cu containing phases such as Ca-Cu-Si were also observed by XRD spectra as also confirmed by other researchers. It was observed that leaching of Cu (II) was lower in CBPC-50 composites, even though the CBPC-50 binder had nearly 4 times greater concentrations of Cu (II) in comparison to the CBPC-5 composites. It represents the formation of an additional binder phase resulting due to the reaction of adsorbed Cu (II) on biochar with KH_2PO_4 and hence leading to effective S/S of Cu (II) in CBPC product such as Ca-Cu-Si phases formed in CBPC while stabilization of Cu within CBPC matrix [31, 38]

Table 5. Phases present in phosphate binders used for stabilization of hazardous waste

Sr.No.	Type of cement	Waste added	Amount of waste added (wt. %)	Phases present	Reference
1	Magnesium phosphate cement	Metakaolin	0-50%	Struvite ($MgNH_4PO_4.6H_2O$) Aluminium Silicon oxide	Qin et al. 2020
2	Magnesium phosphate cement	Fly ash	Upto 50%	K-struvite ($MgKPO_4 \cdot 6H_2O$), $AlKO_6Si_2$	Liu and Yang, 2018
3	Phosphate enhanced calcium aluminate cement	Municipal solid waste ash	Upto 90%	Gibbsite, calcium aluminium oxide, $NaPb_4(PO_4)_3$	Chen et al. 2021
4	Magnesium phosphate cement	Fly ash and metakaolin	30-50 %	K-struvite, periclase, mullite	Lv et al. 2019
5	Calcium sodium phosphate and magnesium potassium phosphate	Mercury contaminated waste ash	25, 50%	$MgKPO_4 \cdot 6H_2O$ (K-struvite) and CaNaPO4	Cho and Lee, 2014
6	Calcium potassium phosphate cement	Canola meal bioachar	10-50%	K-struvite ($MgKPO_4 \cdot 6H_2O$), $CaNaPO_4$, Ca-As-O	Devi and Kothari, 2019
7	Calcium potassium phosphate cement	Pine cone spent biochar	5-50%	K-struvite ($MgKPO_4 \cdot 6H_2O$), $Cu_3(PO_4)_2$, Ca-Cu-Si	Present study

Struvite or K-struvite is considered as a basic building block which links the particles of magnesia and enhances the compaction of the CBPC structure and imparts strength. The characteristic peaks of magnesium silicate were observed by XRD [39, 42] (etc., (Table 5). Some researchers present a different observation suggesting the formation of $AlKO_6Si_2$ structure in the secondary hydration [40] (Table 5). In previous research, precipitation of stable heavy metal phosphates has been confirmed for e.g., Chen et al. [41] showed the

formation of lead phosphate precipitates (K_{sp}=7.9×10−43 at 25 °C) and various different lead phosphate containing phases were formed. Therefore, heavy metal phosphate formed are insoluble and hence prevent the leaching of heavy metals under adverse environmental conditions. The Fig. 6 shows the stabilization of heavy metals by PO_4^{3-} produced during hydration of CBPC. The formation of Cu containing phosphate precipitates ($Cu_3(PO_4)_2$) is confirmed by the XRD spectra of the CBPC product (Fig. 5).

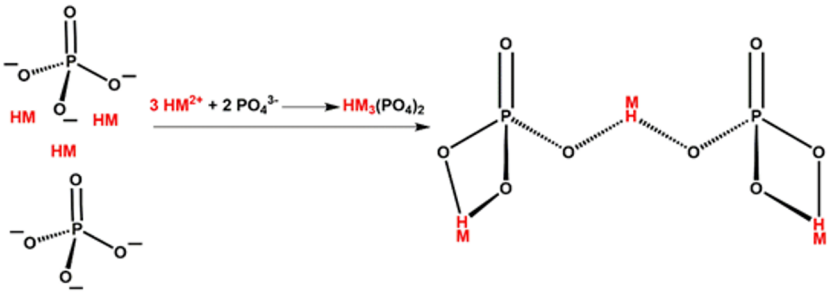

Fig. 6. Stabilization of heavy metal through phosphate ions

3.9 SEM and EDS:

The morphology of the CBPC products was analyzed using Scanning Electron Microscopy (SEM) after carrying out compressive strength test. The fragments of CBPC sample with 25% spent cone biochar were collected and analyzed at various magnification as presented in Fig 7. Cracks were observed in CBPC-25 due to breakage of its structure after compressive strength test. SEM images also confirmed the presence of spent biochar within microcracks and pores of the CBPC matrix [33]. EDS confirmed the presence of Cu in CBPC matrix along with Ca, Si, Al, P etc (Table 6)

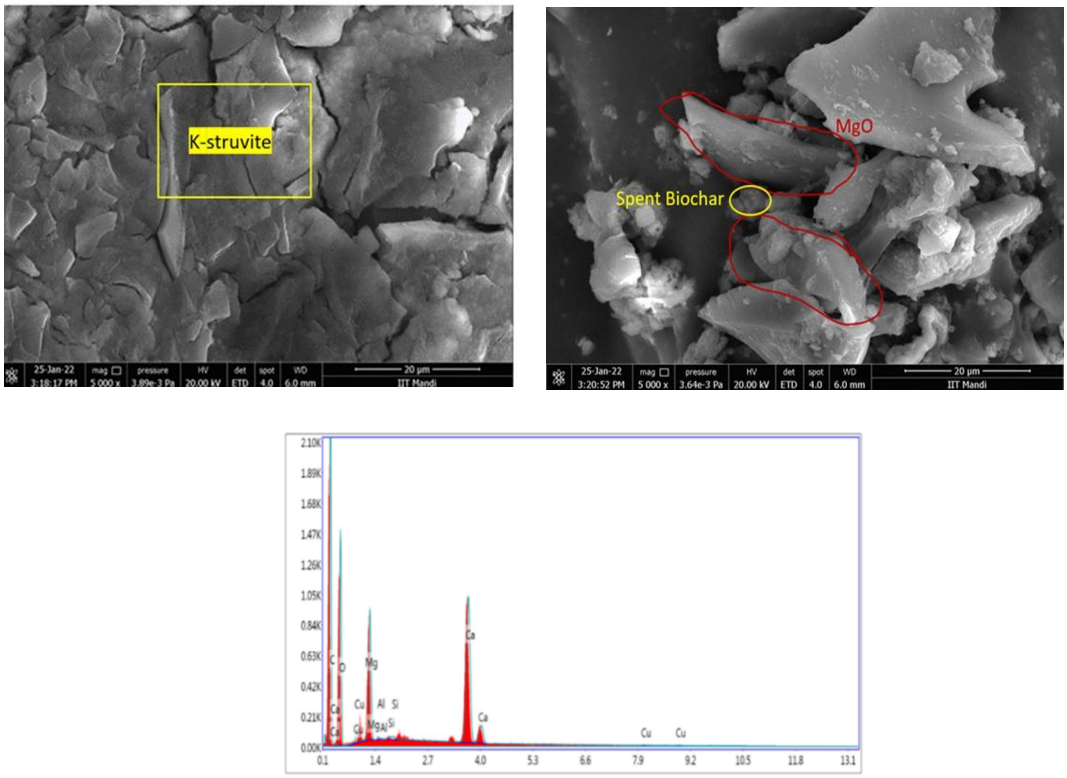

Fig. 7. SEM and EDS analysis CBPC with 25% spent pine cone biochar

Table 6. Elements present after EDS analysis

Element	Weight %	Error %
Ca	11.5	2.34
Si	0.13	37.3
Al	0.08	64.2
Mg	5.75	6.93
Cu	0.24	58
P	3.4	35.2

3.7 Leaching study

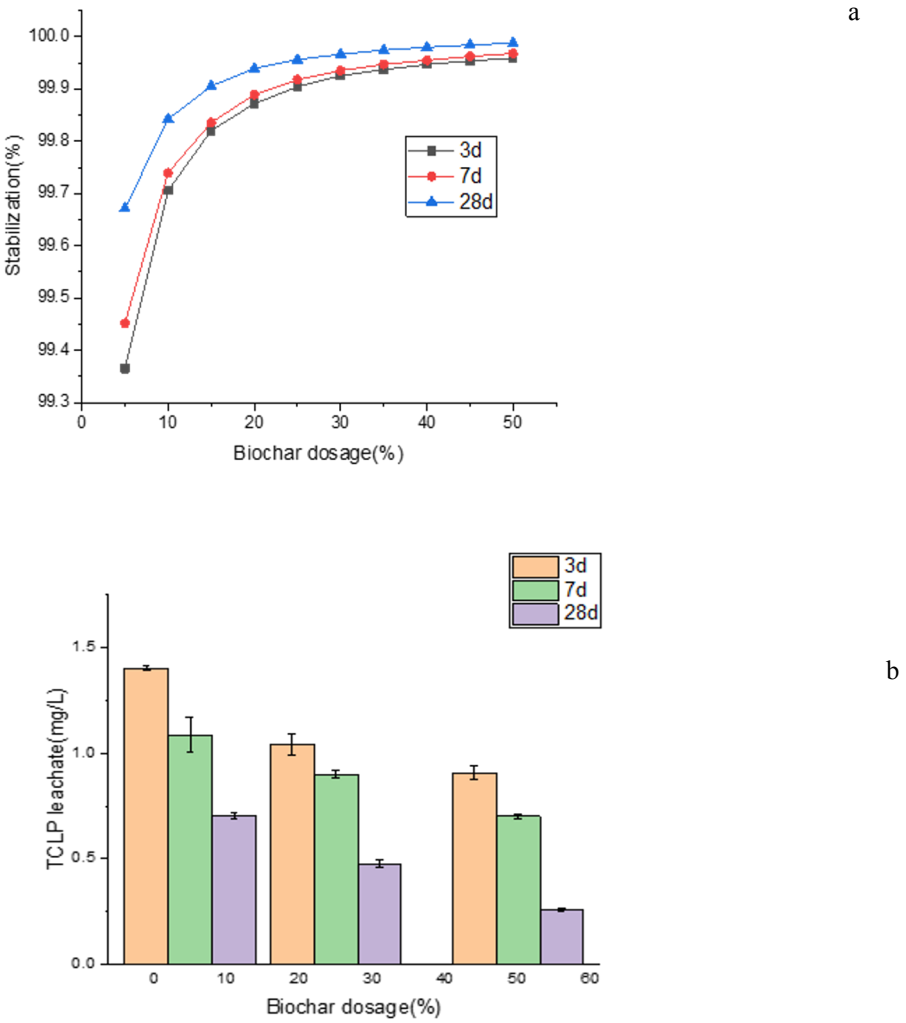

Fig. 8 Effect of biochar content on (a) stabilization (%) (b) concentration of Cu (II) in TCLP leachate

Fig. 8 (a, b) showed the TCLP leachability of Cu (II) from CBPC at different wt. % of spent biochar. The leaching concentration of Cu (II) from CBPC-50 sample was 0.26 mg/ L at 28days (representing 99.8% stabilization efficiency for Cu). Such enhancement in the stabilization efficiency was associated with the precipitation of copper phosphates, such as $Cu_3(PO_4)_2$ as identified in XRD results. The leachate's Cu (II) concentration decreases as the curing time increases, as shown in Figure 8 a.). On the hand, stabilization efficiency (%) increased with increase in curing time (Fig. 8 b). In the majority of the CBPC product leachate, the concentrations of Cu (II) were below the drinking water standards of WHO [27].

3.8 Risk assessment

The assessment of risk to humans is evaluated by determining the possible carcinogenic and non-carcinogenic effects of the leaching of Cu (II) from CBPC product (Fig. 9). The contamination factors (C_f) for CBPC samples with 5-50% spent biochar content are shown in Table 7. As shown in Table 7, there was a decrease in the C_f values of Cu (II) from 0.047 to 0.008, with an increase in the biochar content from 5 -50 wt. %. It depicts that there was a significant reduction in the heavy metal contamination of CBPC product at high biochar concentration. The leaching potential was minimum in CBPC product at 50%. The non-carcinogenic assessment of risk was observed on the basis of exposure to heavy metals by direct contact with leachate through touch or skin or due to ingestion. The value of $EA_{Ingestion}$ was found to be higher than that of EA_{Dermal} suggesting that the major path for exposure to heavy metals was through ingestion in all the samples. There was a decrease in $EA_{Ingestion}$ with increase in biochar content as follows: CBPC-10 > CBPC-25 > CBPC-50. Also, the value of $HQ_{Ingestion}$ / Dermal was found to be in the decreasing order as follows: CBPC-5 > CBPC-25 > CBPC-50. Table 6 depicts the HI for Cu (II) through 2 different pathways i.e., Ingestion and dermal. It can be seen that the risk from ingestion of Cu (II) is nearly 1.5 times greater than through dermal pathway. The average values for HI of CBPC product was found to be well within the permissible limits. The values for $HI_{Ingestion}$ and HI_{Dermal} were found to be less than 1, which clearly depicted that there was no significant danger due to potential leaching of Cu (II). Hence, CBPC product can be readily used in landfills as there is no significant danger of Cu (II) leaching into groundwater.

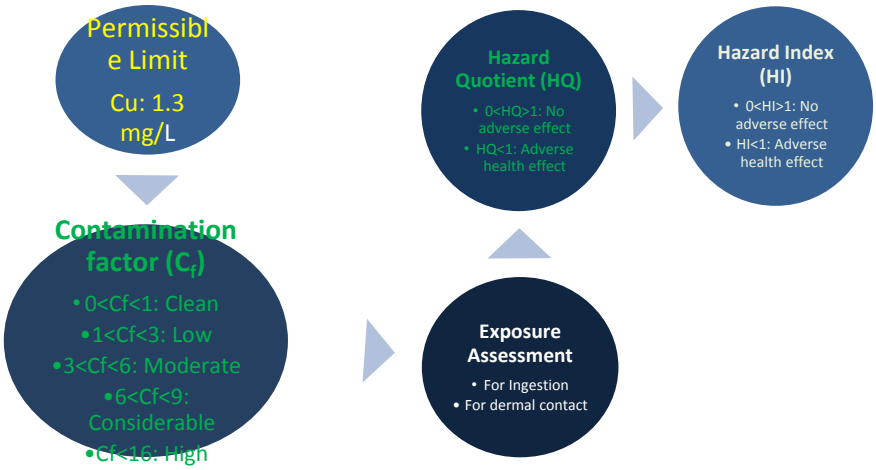

Fig. 9 Flow chart of risk assessment studies

Table 7. Risk assessment analysis of CBPC samples with varying biochar concentration:

Biochar Content (%)	C_{total}	$C_{leachate}$	C_f	C (mg/Kg)	$E_{ingestion}$	E_{dermal}	$HQ_{ingestion}$	HQ_{dermal}	$HI_{ingestion}$	HI_{dermal}
5	43.8	2.1	0.04794	1095	0.0017833	6.2415E-06	6.035665714	5.0001248	1.961614286	8.00686565
25	219	4	0.01826	5475	0.0089164	3.1208E-05	3.178328571	2.0006242		
50	438	3.5	0.00799	10950	0.0178329	6.2415E-05	0.356657143	0.0012483		

3.9 Comparison with previous literature:

The CPBC product used for S/S of heavy metal laden biochar was compared with various different binders such as OPC, geopolymers, cement stabilized with nanoparticles, and thermal treatment (Table VII). As shown in Table 8, CBPC showed a good performance with reduced leaching of heavy metals in comparison with other binders. The order of leaching after TCLP experiments from the final product is in the following order: Thermal treatment < CBPC product < geopolymer < portland cement < nanoparticles stabilized cement. Treatment with cement and Thermal Treatment are regarded as the most efficient methods for S/S of heavy metals because of their ability to form a dese and a highly durable binder phase to encompass these heavy metals. Thermal treatment requires a very high temperature for efficient and effective S/S of heavy metal which is considered as a drawback for the use of Thermal Treatments. As such the most common binders used for S/S of heavy metals are generally cement based. They also have their drawbacks and one of the major concerns is the leaching of heavy metals from these matrices in acidic conditions. To overcome this, adsorbents based on nano particles are added to cement which prevent the oxidation of metal ions in such environments and thus reduce the leaching from the matrix [43]. In the present study, CPBC product showed a higher degree of immobilization for Cu, as can be seen from the leaching values. This value of Cu in CBPC product (0.26 mg/L) was significantly lower than that of cement (0.74 mg/L) [20, 44]. It can be attributed to the fact that a reaction between heavy metal and the binder material taken place which leads to formation of metal containing phases.

Table 8. Comparison with previous studies using different binders

Binding technique	**Heavy metal**	**Waste**	**Heavy metal content**	**Phase**	**Compressive strength (MPa)**	**TCLP value**	**References**
Geopolymerization	Cr	Biochar ofpPaper mill sludge	7.9mg/kg 147.3mg/kg 19.0mg/kg 332.5mg/kg 48.5mg/kg 1.8 mg/kg	Sodium aluminum silicate	Upto 18	0.4 mg/L	Devi and Saroha, 2014
Nanoparticles stabilized cement	Cr	Tannery sludge	24.2 g/kg	$FeCr_2O_4$ and $Cr_{1.3}Fe_{0.7}O_3$	0.5	0.76 mg/L	Arthy and Phanikumar (2017)
Thermal treatment	Mo	Industrial sludge	33 mg/Kg	Magnetite Plagioclase Clinopyroxn	5-12	0.0002 mg/L	Verbinnen et al. 2015
Ordinary portland cement (OPC)	As	Adsorbent sludge	0.3 mg/g	Calcium hydroxide arsenate	28	0.74 mg/L	Kundu and Gupta (2008)
Chemically bonded phosphate cement (CBPC)	Cu (II)	Spent pine cone adsorbent	21.9 mg/g	$MgKPO_4$	13	0.26 mg/L	Present study

4 Conclusions

The research conducted focused on the solidification and stabilization of spent pine cone biochar using a binder called Calcium-Based Phosphate Cement (CBPC). The aim was to determine the most suitable binder and optimize the compressive strength of the resulting product for the purpose of immobilizing copper-loaded biochar.

Three different binders were tested: KH_2PO_4, NaH_2PO4, and (NH_4) H_2PO_4. Among these, KH_2PO_4 in a weight ratio of 1:1:1 was identified as the most suitable binder, exhibiting the highest compressive strength of 10.8 MPa and lowest water absorption after a curing time of 28 days. The research then proceeded to combine CBPC with spent pine cone biochar, by increasing biochar content up to 50%. The CBPC with 25% of spent pine-cone biochar achieved the highest compressive strength of 12.8 MPa at a curing time of 28 days, with a water to solid (W:S) of 0.18.

Leaching studies were conducted using the Toxicity Characteristic Leaching Procedure (TCLP), which showed that CBPC-50 had the lowest leaching potential despite the high content of spent biochar. This suggests that the immobilization of copper-loaded biochar using CBPC effectively reduces the leaching of heavy metals. Microscopic analysis through scanning electron microscopy (SEM) and X-ray diffraction (XRD) confirmed the presence of K-struvite and copper-containing phases such as Ca-Cu-Si in the final CBPC product. An assessment of the risk and leaching potential indicated that the leaching of heavy metals from the CBPC product poses no significant risk to the environment. This finding is important in terms of environmental safety and potential applications of the CBPC product.

Based on the findings of this research, it can be concluded that the final CBPC product, with an optimum compressive strength of 12.8 MPa, exceeds the minimum requirement of 3.5 MPa set by the US Nuclear Regulatory Commission Standard. This indicates that the CBPC with spent pine-cone biochar demonstrates excellent strength properties, making it a viable option for immobilization purposes. Furthermore, the conducted leaching and risk assessment studies provide additional support for the suitability of the CBPC product. The leaching study using the Toxicity Characteristic Leaching Procedure (TCLP) revealed that CBPC-50 exhibited the lowest leaching potential, even with a relatively high content of spent biochar. This implies that the CBPC effectively immobilizes heavy metals, such as copper, present in the biochar, reducing the risk of environmental contamination. Based on these findings, it can be inferred that the final CBPC product is a safe material for disposal. The risk assessment conducted demonstrates that the leaching of heavy metals from the CBPC product poses no significant threat to the environment. Therefore, the final CBPC product can be disposed of in hazardous landfill sites without posing a hazard to the surrounding environment.

Overall, the research findings suggest that CBPC with spent pine-cone biochar can be considered as a suitable and effective immobilization technique for the treatment and disposal of copper-loaded biochar. Its ability to exceed the compressive strength requirement and demonstrate low leaching potential supports its potential application in waste management and environmental remediation practices.

Data availability statement:

The authors confirm that the data supporting the findings of this study are available within the article and its supplementary materials.

Competing interest statement:

The authors have no competing interests to declare that are relevant to the contents of this article.

References:

1. V. Baskar, N. Bolan, S. A. Hoang, P. Sooriyakumar, M. Kumar, L. Singh, & K. H. Siddique. Recovery, regeneration and sustainable management of spent adsorbents from wastewater treatment streams: A review. *Sci. Total Environ.*, **822**:153555 (2022).
2. Pohl. Removal of heavy metal ions from water and wastewaters by sulfur-containing precipitation agents. *Water Air Soil Pollut.*, ***231***(10), 1-17 (2020).
3. Bashir, L. A. Malik, S. Ahad, T. Manzoor, M. A. Bhat, G. N. Dar, & A. H. Pandith. Removal of heavy metal ions from aqueous system by ion-exchange and biosorption methods. *Environ. Chem. Lett.*, ***17***(2), 729-754 (2019).
4. W. S. Chai, J. Y. Cheun, P. S. Kumar, M. Mubashir, Z. Majeed, F. Banat, & P. L. Show. A review on conventional and novel materials towards heavy metal adsorption in wastewater treatment applicationJ. Clean. Prod., ***296***, 126589 (2021).
5. N. A. Qasem, R. H. Mohammed, & D. U. Lawal. Removal of heavy metal ions from wastewater: A comprehensive and critical review. *Npj Clean Water*, ***4***(1), 1-15 (2021).
6. S. Tyagi, M. Bashir, C. Mohan, & A. Annachhatre. Characterization of Pine Residues from Himalayan Region and Their Use as Copper Adsorbent. *Water Air Soil Pollut.*, ***233***(6), 1-24 (2022).
7. P. O. Oladoye. Natural, low-cost adsorbents for toxic Pb (II) ion sequestration from (waste) water: A state-of-the-art review. *Chemosphere*, ***287***, 132130 (2022).
8. Z. Liu, Z. Wang, H. Chen, T. Cai, & Z. Liu. Hydrochar and pyrochar for sorption of pollutants in wastewater and exhaust gas: A critical review. *Environ. Pollut.*, ***268***, 115910 (2021).
9. F. Liao, L. Yang, Q. Li, Y. R. Li, L. T. Yang, M. Anas, & D. L. Huang. Characteristics and inorganic N holding ability of biochar derived from the pyrolysis of agricultural and forestal residues in the southern China. *J Anal Appl Pyrolysis*, ***134***, 544-551 (2018).
10. M. Bashir, C. Mohan, S. Tyagi, & A. Annachhatre. Copper removal from aqueous solution using chemical precipitation and adsorption by Himalayan Pine Forest Residue as Biochar. *Water Sci. Technol.*, ***86***(3), 530-554 (2022).
11. M. K. Yadav, D. Saidulu, P. S. Ghosal, A. Mukherjee, & A. K. Gupta. A review on the management of arsenic-laden spent adsorbent: Insights of global practices, process criticality, and sustainable solutions. *Environ. Technol. Innov.*, ***27***, 102500 (2022).
12. T. S. Singh, & K. K. Pant. Solidification/stabilization of arsenic containing solid wastes using portland cement, fly ash and polymeric materials. *J. Hazard. Mater.*, ***131***(1-3), 29-36 (2006).
13. Y. Wang, F. Han, & J. Mu. Solidification/stabilization mechanism of Pb (II), Cd (II), Mn (II) and Cr (III) in fly ash based geopolymers. *Constr Build Mater.*, ***160***, 818-827 (2018).
14. Guo, B. Liu, J. Yang, & S. Zhang, The mechanisms of heavy metal immobilization by cementitious material treatments and thermal treatments: A review. *J. Environ. Manage.*, ***193***, 410-422 (2017).
15. H. Yoon, D. H. Moon, K. W. Kim, K. Y. Lee, J. H. Lee, & M. G. Kim. Mechanism for the stabilization/solidification of arsenic-contaminated soils with Portland cement and cement kiln dust. *J. Environ. Manage.*, ***91***(11), 2322-2328 (2010).
16. Xu, B. Lothenbach, A. Leemann, & F. Winnefeld. Reaction mechanism of magnesium potassium phosphate cement with high magnesium-to-phosphate ratio. *Cem Concr Res* .***108***, 140-151 (2018).

17. F. Qiao. Reaction mechanisms of magnesium potassium phosphate cement and its application. Dissertation Abstracts International, ***226*** ISBN: 9781267848444 (2010).
18. M. A. Haque, & B. Chen. Research progresses on magnesium phosphate cement: A review. *Constr Build Mater.*, ***211***, 885-898 (2019).
19. X. Cao, R. Ma, Q. Zhang, W. Wang, Q. Liao, S. Sun, & X. Liu. The factors influencing sludge incineration residue (SIR)-based magnesium potassium phosphate cement and the solidification/stabilization characteristics and mechanisms of heavy metals. *Chemosphere*, ***261***, 127789 (2020).
20. W. Y. Xia, Y. S. Feng, F. Jin, L. M. Zhang, & Y. J. Du. Stabilization and solidification of a heavy metal contaminated site soil using a hydroxyapatite-based binder. *Constr Build Mater.*, ***156***, 199-207 (2017).
21. J. H. Cho, Y. Eom, & T. G. Lee, Stabilization/solidification of mercury-contaminated waste ash using calcium sodium phosphate (CNP) and magnesium potassium phosphate (MKP) processes. *J. Hazard. Mater.*, ***278***, 474-482 (2014).
22. S. Ahmad, R. A. Khushnood, P. Jagdale, J. M. Tulliani, & G. A. Ferro. High performance self-consolidating cementitious composites by using micro carbonized bamboo particles. *Mater. Des.*, ***76***, 223-229 (2015).
23. R. A. Khushnood, S. Ahmad, L. Restuccia, C. Spoto, P. Jagdale, J. M. Tulliani, & G. A. Ferro. Carbonized nano/microparticles for enhanced mechanical properties and electromagnetic interference shielding of cementitious materials. *Front. Struct. Civ.*, *10*(2), 209-213 (2016).
24. P. Devi, & A. K. Saroha. Risk analysis of pyrolyzed biochar made from paper mill effluent treatment plant sludge for bioavailability and eco-toxicity of heavy metals. *Bioresour. Technol.*, *162*, 308-315 (2014).
25. S. Zhang, S. Dai, R. B. Finkelman, I. T. Graham, D. French, J. C. Hower, & X. Li, Leaching characteristics of alkaline coal combustion by-products: A case study from a coal-fired power plant, Hebei Province, China. *Fuel*, ***255***, 115710 (2019).
26. Z. Banu, M. S. A. Chowdhury, M. D. Hossain, & K. I. Nakagami, Contamination and ecological risk assessment of heavy metal in the sediment of Turag River, Bangladesh: an index analysis approach. *J. water resource prot.* ***5****(2),* 28446 (2013).
27. Kumar, M., & Puri, A. A review of permissible limits of drinking water. *Indian J. Occup*, ***16***(1), 40 (2012).
28. USEPA, Risk Assessment Guidance for Superfund, volume1, Human Health Evaluation Manual (Part A). Report EPA/540/1–89/002. US Environmental Protection Agency, Washington, DC (1989).
29. USEPA, Risk Assessment Guidance for Superfund, Volume 1, Human Health Evaluation Manual (Part E, Supplemental Guidance for Dermal Risk Assessment). Report EPA/540/R/99/005. US Environmental Protection Agency, Washington, DC (2004).
30. C. X. Qian & J. M. Yang, Effect of disodium hydrogen phosphate on hydration and hardening of magnesium potassium phosphate cement. *J. Mater. Civ. Eng.*, ***23***(10), 1405-1411 (2011).
31. P. Devi, P. Kothari, & A. K. Dalai, Stabilization and solidification of arsenic and iron contaminated canola meal biochar using chemically modified phosphate binders. *J. Hazard. Mater.*, ***385***, 121559 (2020).
32. Y. Li, T. Shi, & B. Chen. Experimental study of dipotassium hydrogen phosphate influencing properties of magnesium phosphate cement. *J. Mater. Civ. Eng.,* ***28***(4), 04015170 (2016).
33. J. Shu, L. Cai, J. Zhao, H. Feng, M. Chen, X. Zhang, & R. Liu. A low cost of phosphate-based binder for Mn^{2+} and NH_4^+-N simultaneous stabilization in electrolytic manganese residue. *Ecotoxicol.*, ***205***, 111317 (2020).

34. M. R. Ahmad, B. Chen, & H. Duan. Improvement effect of pyrolyzed agro-food biochar on the properties of magnesium phosphate cement. *Sci. Total Environ.*, ***718***, 137422 (2020).
35. H. T. Kim, & T. G. Lee. A simultaneous stabilization and solidification of the top five most toxic heavy metals (Hg, Pb, As, Cr, and Cd). *Chemosphere*, ***178***, 479-485 (2017).
36. H., Moon, D. Dermatas, & N. Menounou, (2004). Arsenic immobilization by calcium–arsenic precipitates in lime treated soils. *Sci. Total Environ.*, ***330***(1-3), 171-185.
37. W. Wanmolee, N. Sosa, A. Junkaew, S. Youngjan, C. Geantet, P. Afanasiev, & P. Khemthong. Phase speciation and surface analysis of copper phosphate on high surface area silica support by in situ XAS/XRD and DFT: Assessment for guaiacol hydrodeoxygenation. *Appl. Surf. Sci.*, ***574***, 151577 (2022).
38. M. Rizwan, M. Z. ur Rehman, S. Ali, T. Abbas, A. Maqbool, & A. Bashir Biochar is a potential source of silicon fertilizer: An overview. Biochar from biomass and waste, 225-238, ISBN: 9780128117293 (2019).
39. S. Wagh, S. Y. Jeong, & D. Singh, High strength phosphate cement using industrial byproduct ashes. In *Proceedings of the 1st International Conference on High Strength Concrete*, 542-553 (1997).
40. Z. Qin, C. Ma, Z. Zheng, G. Long, & B. Chen. Effects of metakaolin on properties and microstructure of magnesium phosphate cement. *Constr Build Mater.* ***234***, 117353 (2020).
41. R. Liu, Y. Yang, & S. Sun, Effect of M/P and borax on the hydration properties of magnesium potassium phosphate cement blended with large volume of fly ash. *J. Wuhan Univ. Technol. Mater. Sci. Ed.*, ***33***(5), 1159-1167 (2018).
42. L. Chen, Y. S. Wang, L. Wang, Y. Zhang, J. Li, L. Tong, & D. C. Tsang. Stabilisation/solidification of municipal solid waste incineration fly ash by phosphate-enhanced calcium aluminate cement. *J. Hazard. Mater.*, ***408***, 124404 (2021).
43. L. Lv, P. Huang, L. Mo, M. Deng, J. Qian, & A. Wang. Properties of magnesium potassium phosphate cement pastes exposed to water curing: A comparison study on the influences of fly ash and metakaolin. *Constr Build Mater.*, **203**, 589-600 (2019).
44. M. Arthy, & B. R. Phanikumar. Solidification/stabilization of tannery sludge with iron-based nanoparticles and nano-biocomposites. *Environ. Earth Sci*, ***76***(4), 1-17 (2017).
45. Verbinnen, C. Block, J. Van Caneghem, & C. Vandecasteele. Recycling of spent adsorbents for oxyanions and heavy metal ions in the production of ceramics. *Waste Manage.*, ***45***, 407-411 (2015).